Microwave ablation of liver tumors: degree of tissue contraction as compared to RF ablation

Jeong Kyong Lee,[1,4] Surachate Siripongsakun,[1,3] Simin Bahrami,[1] Steven S. Raman,[1] James Sayre,[1,2] David S. Lu[1]

[1]Department of Radiology, David Geffen School of Medicine at UCLA, Los Angeles, CA, USA
[2]Department of Biostatistics, School of Public Health, UCLA, Los Angeles, CA, USA
[3]Department of Radiology, Chalubhorn Hospital, Bangkok, Thailand
[4]Department of Radiology, Ewha Womans University, Seoul, Korea

Abstract

Purpose: To compare the amount of tissue contraction after microwave (MW) versus radiofrequency (RF) ablation of liver tumors.
Materials and methods: Seventy-five hepatic tumors in 65 patients who underwent percutaneous MW or RF ablations were included in this retrospective study. All patients underwent MRI within 6 months before the ablation and 24 h after the procedure. Two blinded radiologists, by consensus, performed measurements on the corresponding series of pre and post-ablation MRI. Absolute and relative contraction of liver, tumor, and control were calculated and compared.
Results: Thirty-one patients underwent MW ablations, and 44 patients underwent RF ablations. The absolute and relative contraction of the ablation zone were significantly greater with MW than RF ablation ($p = 0.003$ to < 0.001). Thirty-two lesions were visible on both pre- and post-ablation MRI. MW ablation had significantly more tumor contraction as compared to RF ablation ($p = 0.003$ to 0.009). The control measurements demonstrated no significant difference in normal tissue variation between MW and RF groups.
Conclusions: MW ablation of hepatic tumors produced significantly more contraction of tumor and ablated hepatic tissue compared to RF ablation. Tissue contraction should be taken into account during pre-procedural planning and assessing treatment response by comparing pre- and post-ablation images.

Microwave (MW) ablation is a promising technique for the local treatment of hepatic tumors. MW is not as well established as radiofrequency (RF) ablation, and the applications of MW are limited in some countries. A potential advantage of MW over RF ablation in the treatment of large tumors is the ability to create a more extensive ablation zone [1–4].

Several studies have reported that ablated tissues shrink on imaging immediately after RF ablation possibly as a result of protein denaturation, contraction of collagen, and dehydration [5–8]. Recently, a laboratory study using ex vivo bovine liver demonstrated that MW ablation zones contracted more than RF ablation zones immediately after the procedure [8]. The contraction of ablated tissue on immediate post-ablation imaging leads to the underestimation of the original ablation zone size. In the clinical setting, the ablation method and device are chosen based on the expected ablation zone size. The ablation zone size is critical in pre-procedural planning and assessing treatment response. Therefore, the contraction of tissue should be taken into account for appropriate assessment of the ablation zone if MW ablation causes significantly more contraction than RF ablation.

To the best of our knowledge, there are no published in vivo human liver data on tissue contraction resulting from MW ablation. The purpose of this study is to compare the amount of tissue contraction caused by MW versus RF ablation in a cohort of patients with hepatic tumors.

Correspondence to: David S. Lu; *email:* dlu@mednet.ucla.edu

Materials and methods

Patients

Our study was compliant with the Health Insurance Portability and Accountability Act (HIPAA) and was approved by the institutional review board. The need for obtaining signed informed consent was waived for this retrospective analysis. Between January 2010 and May 2012, seventy-five liver lesions in 65 patients who underwent MW or RF ablation of hepatic malignancy with original tumor size ranging from 1 to 6.5 cm in diameter and had MR imaging before and after the ablations were included in this study. MR imaging was performed within 6 months before the ablation and within 24 h after the ablation. Medical records of all patients were reviewed for demographic and clinical data.

MR imaging

Only images of adequate quality meeting set minimal standards were included in this study. These consisted of multiphasic pre- and post-gadolinium-enhanced MRI on 1.5T and 3.0T scanners using body phase-array coils. Sequences included axial T2-weighted multi-shot and/or single-shot techniques, T1-weighted in-phase and opposed-phase gradient echo, and pre- and post-gadolinium contrast-enhanced T1-weighted 2D or 3D gradient echo with or without fat suppression. The post-contrast sequences consisted of multiphasic acquisitions during the late arterial, portal venous, and at least one additional delayed venous phase, with section thickness of 6–8 mm for 2D acquisition on earlier generation scanners and 2.5–5 mm for 3D acquisition on later generation scanners. MR images were excluded when there were no reliable liver landmarks for measurements by consensus of the readers and when images were of unacceptable quality.

Ablation technique

All ablations were performed under general anesthesia with real-time ultrasound and/or CT guidance.

MW ablation was performed percutaneously or during laparotomy using 17-gauge gas-cooled triaxial antennae (Certus 140, LK 15; NeuWave Medical, Madison, Wisconsin) delivering power from a 2.45-GHz generator with maximum output of 140-W, or 13-gauge water-cooled dipole antennae (Evident; Valleylab, Boulder, Colorado) coupled to a 915-MHz generator with maximum output power of 45-W.

RF ablation was performed percutaneously using single or cluster 17-gauge internally cooled electrodes (Cool-tip; Valleylab, Boulder, Colorado). RF power was delivered using an impedance-based pulsing algorithm with a maximum 200-W generator output.

Measurement details

Two authors (S.S. and S.B., with 3 and 4 years of experience in liver MR, respectively), blinded to clinical information and ablation type, performed all image selections and measurements in consensus. They selected the best MR sequence depicting each tumor and the subsequent ablation zone in pre- and post-ablation images. Using this MR sequence, the best matched pre- and post-ablation images of the tumor and ablation zone were selected for tissue measurements. The commonly used sequences were the following: portal venous phase T1WI, hepatobiliary phase of T1WI (if hepatocyte-specific contrast agent was used), and T2WI.

Next, internal hepatic structures (e.g., vascular or bile duct branching points nearest to the index tumor and ablation zone) and liver surface landmarks (e.g., fixed indentation of the liver surface) which matched on the selected pre- and post-ablation MR images were chosen as the reference points for measurements. Distances were measured between either two internal hepatic reference points or one internal hepatic reference and one surface landmark. If multiple appropriate reference points were present, the shortest distance was chosen first. The measurements were performed using manually positioned electronic calipers directly on picture archiving and communication system. Readers performed each measurement twice by consensus, and the average was used for analysis.

Measured values were as follows: (1) pre-ablation distance was the shortest distance between two hepatic reference points which passed through the index tumor on the pre-ablation image (Fig. 1A and B); (2) post-ablation distance was the shortest distance between the two reference points used for the pre-ablation distance which passed through the ablation zone on the post-ablation image (Fig. 1C and D), and this measurement line had to include more ablation zone than normal liver; (3) ablation zone size was the distance occupied by the ablation zone in the post-ablation distance; (4) pre-ablation tumor size was the diameter of the index tumor on the pre-ablation image (Fig. 2A); (5) post-ablation tumor size was the diameter of the index tumor on the post-ablation image when the outline of the ablated tumor was still visible within the ablation zone (Fig. 2B); (6) pre-ablation control distance was the shortest distance between two reference points which passed through only normal liver parenchyma (i.e., non-tumor non-ablated liver parenchyma) on the pre-ablation image; and (7) post-ablation control distance was the shortest distance between the two reference points used for the pre-ablation control distance passing through only normal liver parenchyma on the post-ablation image.

Absolute tissue contraction was calculated as follows: (1) absolute ablation zone contraction by subtracting pre-ablation distance from post-ablation distance; (2)
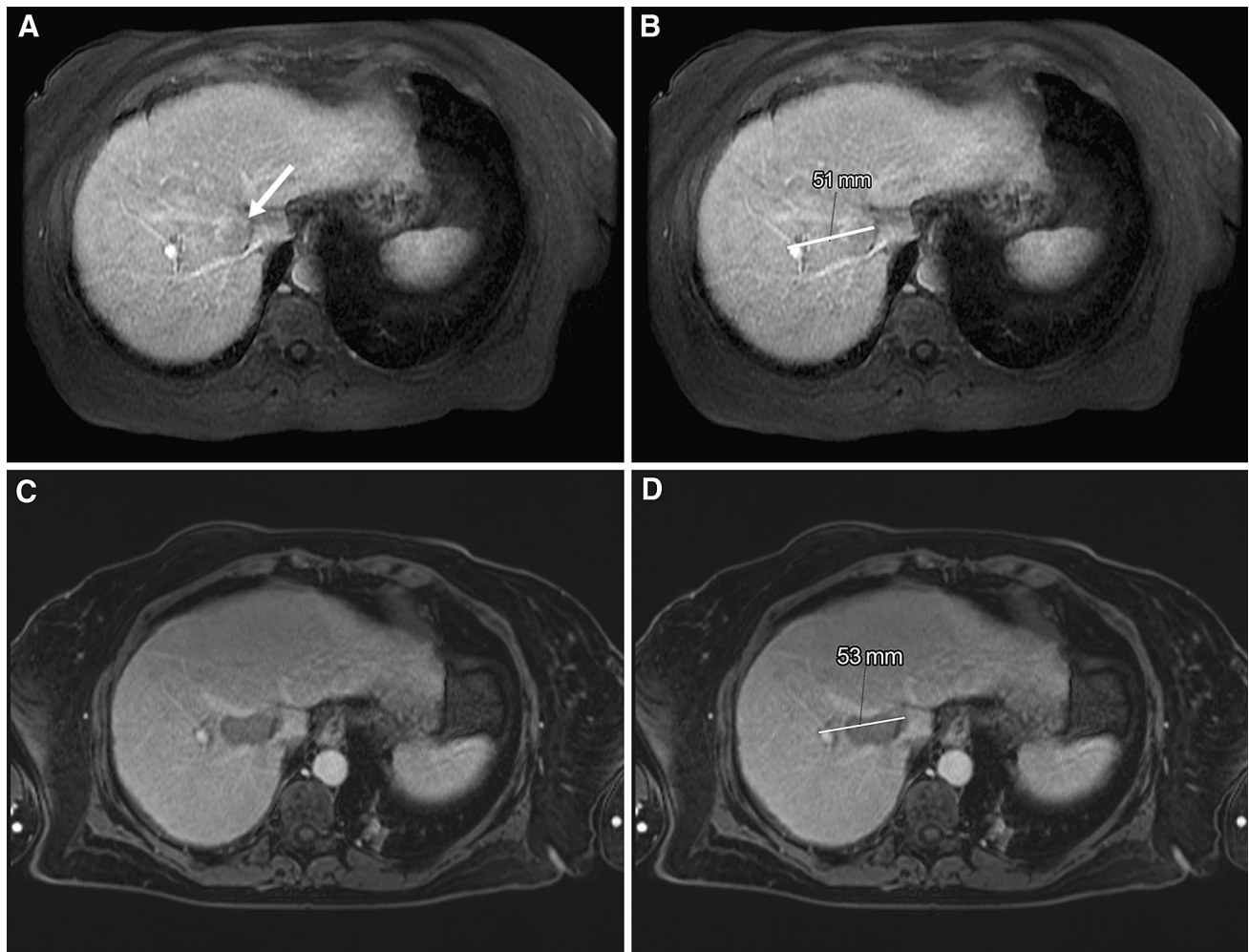
Fig. 1. Measurement method on pre- and post-ablation MRI used to determine liver tissue contraction. **A** Portal venous phase spoiled gradient-echo MR image prior to ablation demonstrates a mass adjacent to the IVC (*arrow*). **B** The same image as **A** showing measurement of pre-ablation distance using two vascular landmarks (distance measured between calipers placed on each landmark). **C** Portal venous phase spoiled gradient-echo MR image immediate after ablation anatomically matched with the pre-ablation MR image (**A**). **D** The same image as **C** showing measurement of post-ablation distance using the same two vascular landmarks as those used on the pre-ablation image (distance between two calipers). Note that the measurement line must pass through more ablation zone than normal liver.

absolute tumor contraction by subtracting pre-ablation tumor size from post-ablation tumor size; and (3) absolute normal liver variation (control) by subtracting pre-ablation control distance from post-ablation control distance.

Relative tissue contraction was calculated as follows: (1) relative ablation zone contraction as $ACaz \bullet 100/Daz$, where $ACaz$ is absolute ablation zone contraction, and Daz is ablation zone size; (2) relative tumor contraction as $ACt \bullet 100/Dt$, where ACt is absolute tumor contraction, and Dt is pre-ablation tumor size; and (3) relative normal liver variation as $ACn \bullet 100/Dn$, where ACn is absolute normal liver variation, and Dn is pre-ablation control distance.

Subgroup analysis was performed between patients with or without liver cirrhosis. Liver cirrhosis was diagnosed based on any MRI morphologic features of liver cirrhosis.

Statistical analysis

The continuous variables were computed using the student t test and analysis of variance (ANOVA). The Chi-square and Fisher exact tests were used for comparing categorical variables. Two-sided p value <0.05 was considered to indicate statistical significance. Statistical software (SPSS, version 20; IBM software Group, New York, NY) was utilized for these calculations.
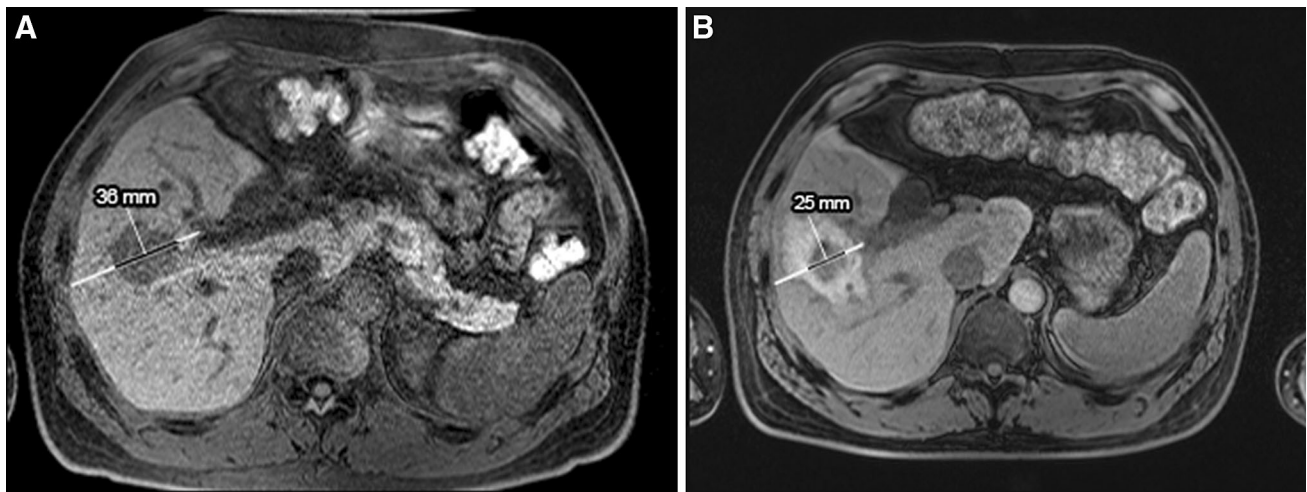
Fig. 2. Tumor contraction after Microwave (MW) ablation of colorectal metastasis. **A** Pre-contrast spoiled gradient-echo T1-weighted MR image prior to MW ablation demonstrates a 3.6-cm hypointense mass in the right lobe of the liver. **B** Pre-contrast spoiled gradient-echo T1-weighted MR image immediate after MW ablation at the same anatomic level as Fig. 4A. This post-ablation MR image shows the contraction of the index tumor which is still visible in the ablation zone after MW ablation. Tumor size decreased from 36 to 25 mm in diameter. Note that the tumor diameter measurement (*black line*) has to be in the same alignment with the ablation zone measurement (*white line*). In this case, relative tumor contraction was calculated as $(36-25) \times 100/36 = -25\%$ (negative value reflecting the decrease in diameter).

Results

Baseline patient characteristics are summarized in Table 1. Thirty-one of 75 lesions received MW ablation and 44 lesions RF ablation for either hepatocellular carcinoma (HCC) or metastasis. The mean age was 65.3 years (range 39–86 years). The mean size of index tumor and ablation zone was 2.5 cm (range 1.0–6.5 cm) and 3.9 cm (range 1.9–8.0), respectively. There was no significant difference between MW and RF ablation groups in terms of age, indications for ablation, and the duration between pre-ablation MR and the ablation. More cirrhotic patients received RF ablation ($p = 0.036$).

The amount of tissue contraction calculated by absolute and relative contraction was significantly greater with MW than RF ablation ($p = 0.003$ to < 0.001; Table 2; Figs. 3, 4). Mean absolute ablation zone contraction was -2.45 mm after MW ablation, which corresponded to -7.1% in relative ablation zone contraction.

There was no significant change in the control measurements of normal liver variation before and after tumor ablation between MW and RF (-0.95 mm vs. $+0.06$ mm contraction, $p = 0.129$). In addition, there was no statistically significant difference between the two groups in terms of elapsed time between the pre-ablation MR and the ablation. Tumors were still visible in the ablation zone on MR images after ablations in 32 (42.7%) patients, consisting of 14 lesions following MW ablation and 18 lesions following RF ablations. More tumor contraction was observed in MW than RF ablations with mean absolute tumor contraction of

Table 1. Baseline characteristics of patients with microwave and radiofrequency ablation

	Ablation method		*p* Value
	Microwave	RFA	
Number of lesions (total patients)	31 (26)	44 (39)	
Age of the patients (Mean ± SD)	62.8 ± 11.4	67 ± 8.9	0.078
Indication for ablation			0.537
Hepatocellular carcinoma	19 (63.1%)	30 (68.2%)	
Metastasis	12 (36.9%)	14 (31.8%)	
Liver status			0.036
Cirrhosis	11 (35.5%)	27 (61.4%)	
Non-cirrhosis	20 (64.5%)	17 (38.6%)	
Duration between pre-ablation MRI and ablation (days)			0.092
Range	2–125	15–106	
Mean ± SD	39 ± 36	50.6 ± 22.8	
Median ± SD	22 ± 36	49.5 ± 22.8	

SD standard deviations

Table 2. Measurements of tissue contraction by Microwave and RF ablation on MRI

	Ablation method		p Value	Calculation method
	Microwave	RFA		
Ablation zone contraction				
Number of lesions	31	44		
Absolute contraction (mm)	-2.45 ± 0.47	0.94 ± 0.38	<0.001	Post-ablation $-$ pre-ablation distance
Relative contraction (%)	-7.11 ± 13.3	2.39 ± 12.7	0.003	$\frac{\text{Absolute contraction} \times 100}{\text{Ablation zone size}}$
Tumor contraction				
Number of lesions	14	18		
Absolute contraction (mm)	-2.37 ± 0.28	0.55 ± 0.26	0.003	Post-ablation $-$ pre-ablation tumor size
Relative contraction (%)	-9.95 ± 10.4	1.31 ± 13.2	0.009	$\frac{\text{Absolute tumor contraction} \times 100}{\text{Pre-ablation tumor size}}$
Control for normal liver variation				
Number of measurements	31	44		
Absolute variation (mm)	-0.95 ± 0.32	0.06 ± 0.18	0.129	Post-ablation $-$ pre-ablation control distance
Relative variation (%)	-1.62 ± 5.85	0.38 ± 4.86	0.11	$\frac{\text{Absolute variation} \times 100}{\text{Pre-ablation distance}}$

The negative results indicate decrease in volume; positive results indicate increasing volume, *RFA* radiofrequency ablation
Data are means ± standard deviations except the number of patients
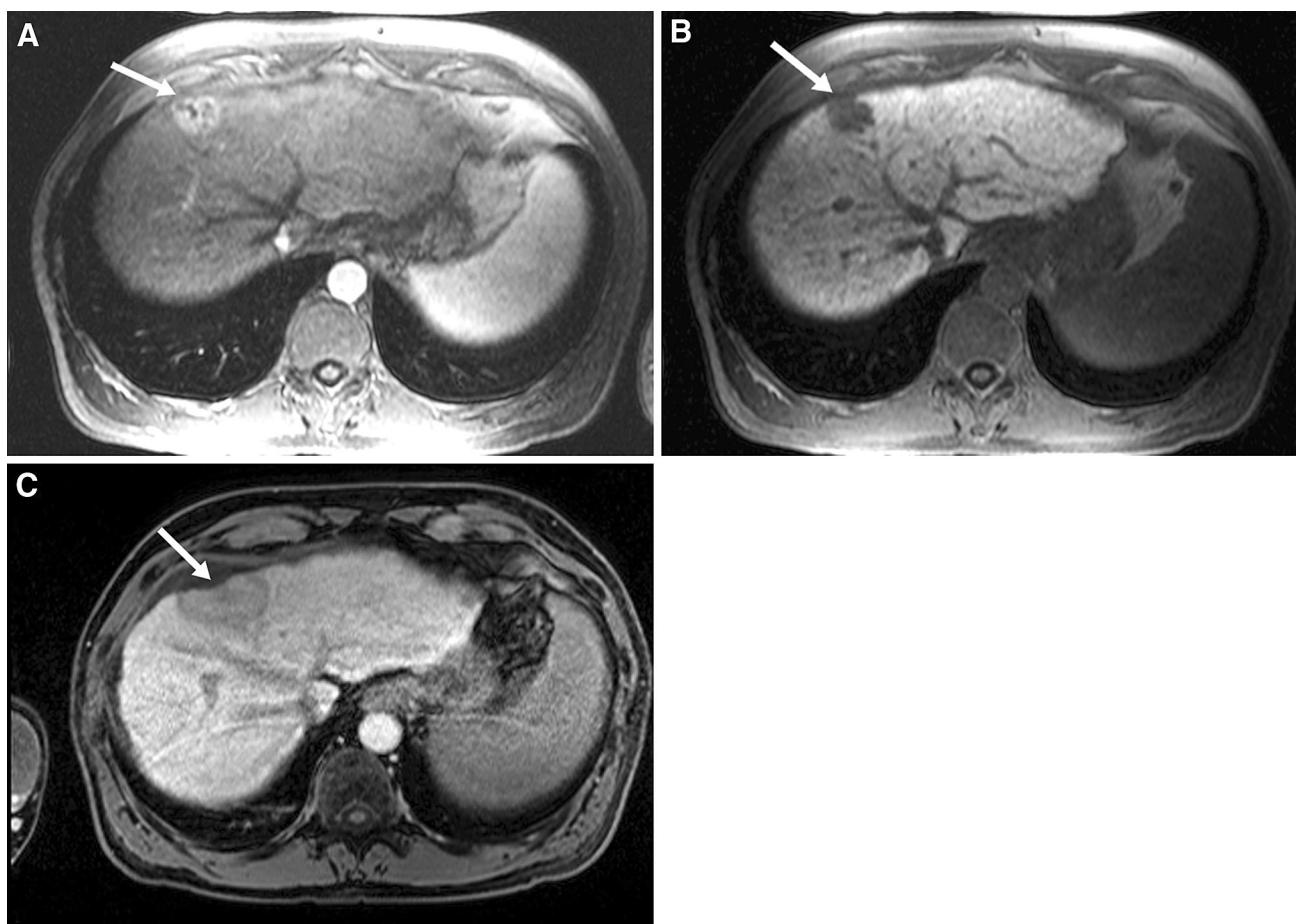
Fig. 3. Liver contraction after microwave (MW) ablation of hepatocellular carcinoma. **A** Arterial phase spoiled gradient-echo T1 weighted MR image shows a 2.5-cm hypervascular hepatocellular carcinoma near the surface of the liver (*arrow*). **B** Hepatobiliary phase spoiled gradient-echo T1-weighted MR image corresponding to Fig. 2A; the mass demonstrates no gadolinium EOB uptake (*arrow*). **C** Five min-delayed phase spoiled gradient-echo T1-weighted MR image after microwave ablation anatomically corresponding to Fig. 2A and B; the post-ablation image clearly demonstrates tissue contraction as evidenced in this case by retraction of the liver capsule at the site of ablation (*arrow*).

-2.37 mm vs. $+0.55$ mm ($p = 0.003$) and relative tumor contraction of -9.95% vs. $+1.3\%$ per cm of tumor ($p = 0.009$) (Table 2; Fig. 2).

In the subgroup analysis of liver cirrhosis and non-cirrhosis, liver metastases were more common than HCC in the non-cirrhotic patients of both RF and MW groups
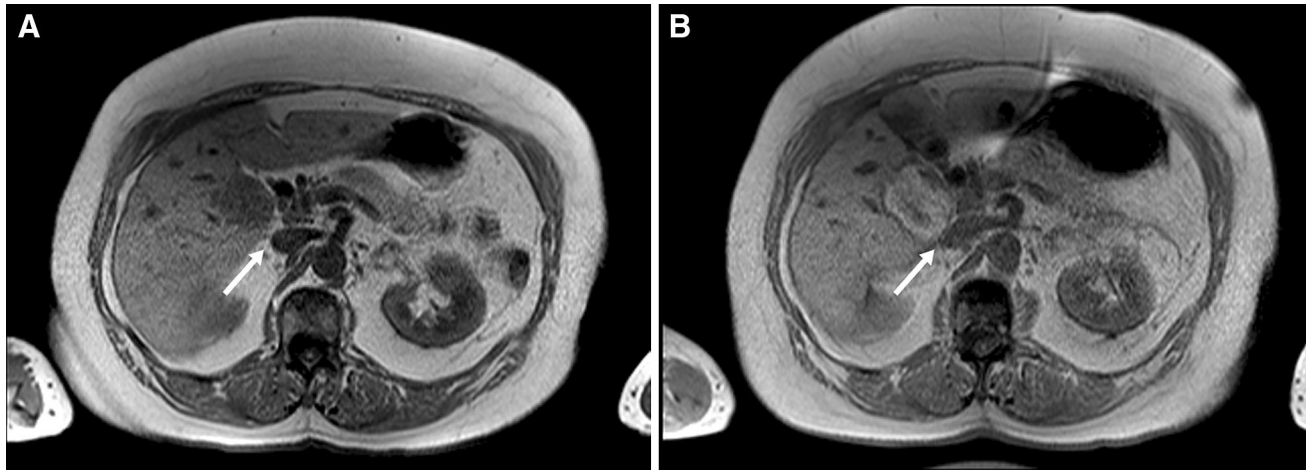
Fig. 4. Effect of radiofrequency (RF) ablation of hepatocellular carcinoma on tissue volume. **A** Pre-contrast spoiled gradient-echo T1-weighted MR image before RF ablation shows a 3.5-cm hypointense mass in proximity to the inferior vena cava (IVC) with a distinct fat plane between the liver surface and the IVC (*arrow*). **B** Pre-contrast spoiled gradient- echo T1-weighted MR image immediately after RF ablation anatomically matched to the MR image in Fig. 3A. This immediate post-ablation MR image demonstrates increased tissue volume at the ablation zone as evidenced in this case by bulging of the liver capsule and effacement of the peri- hepatic fat adjacent to the ablation zone (*arrow*).

Table 3. Subgroups analysis of Microwave and RF ablation according to the presence of liver cirrhosis

	RFA		*p* Value	Microwave		*p* Value
	No cirrhosis	Cirrhosis		No cirrhosis	Cirrhosis	
Number of lesions	17	27		20	11	
Indication for ablation			<0.001			<0.001
Hepatocellular carcinoma	3 (17.6%)	27 (100%)		8 (40%)	11 (100%)	
Metastasis	14 (82.4%)	0		12 (60%)	0	
Ablation zone contraction						
Absolute contraction (mm)	2.2 ± 0.38	0.15 ± 0.37	0.083	−2.5 ± 0.37	−2.9 ± 0.55	0.802
Relative contraction (%)	6.74 ± 12.32	−0.34 ± 12.38	0.071	−6.19 ± 10.25	−8.77 ± 18.12	0.614
Control for normal liver variation						
Absolute variation (mm)	−0.05 ± 0.17	0.02 ± 0.19	0.246	−0.06 ± 0.25	−0.15 ± 0.07	0.443
Relative variation (%)	−0.67 ± 3.86	1.05 ± 5.36	0.258	−1.81 ± 5.89	−1.27 ± 6.03	0.811

The negative results indicate decreasing in volume; positive results indicate increasing volume, *RF* radiofrequency
Data are means ± standard deviations except the number of patients and indication for ablation

($p < 0.001$, Table 3). No significant difference was demonstrated in the control measurement of normal liver variation between cirrhotic versus non-cirrhotic patients in both the groups.

In the RF subgroup, more relative contraction was observed in liver cirrhosis compared to non-cirrhosis with a trend toward statistical significance (−0.34% vs. +6.74%, respectively; $p = 0.07$). In the MW group, there was no significant difference in the tissue contraction between cirrhosis and non-cirrhosis subgroups.

Discussion

MW ablation systems are fundamentally different from RF ablation systems in the way that they heat tissue. [9–11]. MW has several advantages over RF. MW can generate a larger ablation zone in conjunction with less heat-sink effects than RF. MW easily penetrates tissue with high impedance such as lung, bone, and dehydrated or charred tissue [12, 13]. In contrast, MW energy is more difficult to distribute than RF energy and the control of the current available antennae is more challenging due to their larger diameter. The risk of skin burn by excessive power in the antenna shaft is a well-known drawback of MW energy [14, 15], although newer MW systems have addressed this issue to some degree.

Interestingly, Brace et al. reported that tissue contraction by MW ablation is greater than RF ablation in a laboratory study [8]. This may suggest that the true ablation zone created by MW is actually larger than RF although not readily apparent on immediate post-ablation imaging. Thus, we intended to evaluate the degree of tissue contraction caused by MW ablation in patients with hepatic malignancy and compare it with RF ablation using MR imaging.

Our study demonstrates significant tissue contraction following MW ablation; however, the data do not replicate the extent of contraction seen in the prior ex vivo study. In our series, the tissue contraction with MW as calculated by relative ablation zone contraction and relative tumor contraction were only -7.1% and -9.95%, significantly less than the report on explanted bovine liver that demonstrated up to -30% liver contraction.

The most relevant difference between these two studies is that our study reflects in vivo tissue contraction as opposed to non-perfused ex vivo tissue contraction. It has previously been reported that the sizes of ablations are smaller in blood-perfused ex vivo liver than in non-perfused ex vivo liver [16]. Additionally, perfusing ex vivo liver creates an ablation zone size that more closely approximates the ablation size in the in vivo model [16]. It is possible that since the ablation zone size in our series of patients was inherently affected by the perfusion status of the liver tissue, the degree of contraction was similarly affected by perfusion. Another factor is the presence of tumor tissue in our cases. The ex vivo study demonstrated a positive correlation between the water removed and relative contraction for RF and MW ablations in liver [8]. Therefore, in theory, different tissue types will contract to different degrees based on their water content. Inclusion of a larger amount of normal liver parenchyma in our measurements may contribute to the discrepancy between the degrees of tissue contraction. We tried to minimize the inclusion of normal parenchyma by vascular structures nearest to the ablation zone as landmarks. However, to achieve objective accurate measurements despite image differences between pre- and post-ablation MRIs, reliable landmarks were necessary, and thus, the inclusion of a small amount of normal liver parenchyma was inevitable. Other possible explanations include different ablation circumstances used for each patient as opposed to set parameters in the ex vivo study as well as our use of imaging for measurements rather than pathologic samples.

Of note, there has been some controversy in the literature regarding the changes of ablation zone size following RF ablation over time. Two studies exploring this issue utilizing RF ablation data of renal cell carcinoma had conflicting results [5, 17]. One study demonstrated that renal tumors decreased in size up to 21% immediately after RF ablation on CT images with no appreciable change on 1-month follow-up scans [5]. The second study reported approximately 10% increase of RF ablation zones on MR images within the first 2 weeks and involution by an average of 30% within 6 months [17]. Although there may be no conclusive study, some studies suggest that immediate post-ablation imaging can underestimate the true ablation zone size [8, 18, 19].

In our subgroup analysis, HCC was a more common indication than metastases for both ablation methods in the cirrhosis group with statistical significance ($p < 0.001$, Table 3). This finding is as expected since it is reasonable that more HCC than metastases were present in patients with liver cirrhosis.

Considering the distribution of liver cirrhosis, more cases had morphologic features of cirrhosis in the RF ablation group. This likely reflects a selection bias for RF ablation in patients with decreased liver function as MW ablation zones are presumed to be more extensive. Given this difference between the RF and MW ablation groups, we did subgroup analysis based on the absence or presence of liver cirrhosis. Of note, within the subgroup of RF ablation, there was a suggestion of less tissue swelling in cirrhotic livers (-0.34%) as compared to non-cirrhotic livers ($+6.74\%$) based on relative contraction. This approached but did not achieve statistical significance ($p = 0.07$). The trend may reflect the limiting effect of liver fibrosis on the ability of tissue to expand by rehydration following RF ablation. Tissue and tumor type may play a role on the degree of tissue contraction or expansion.

Our study has several limitations that should be noted. Due to the retrospective nature of case collection, the patients included had inhomogeneous data in terms of extent of ablation zone as well as ablation techniques and parameters. To address differences in the timeframe of the pre-ablation MR and clinical history such as liver disease and tumor type, we did subgroup analysis to reveal any effects these factors may have had on our results. Our ablation zone contraction calculations may be underestimating the tissue contraction by including some normal liver parenchyma in the measurement. We addressed this issue by calculating the relative contraction adjusted for the size of the ablation zone and by using the nearest vascular structure identifiable as a landmark to minimize the volume of intervening normal parenchyma. The control measurement of normal liver parenchyma not including ablation zone or tumor was also performed to eliminate the effect of normal liver variation in the time frame between the pre-ablation MRI and the ablation.

Additionally, the measurements were performed by two readers by consensus and inter-observer agreement was not calculated. Also, any sequence of MR could be chosen by readers as long as the ablation zone and landmarks were best visualized. To minimize effects of image variability and for matching pre- and post-ablation images objectively and exactly, two readers had to review images together and decide the same level and location for the measurements. The distances were measured twice, and the average was used for analysis. To further minimize the effect of MR sequences on the data, the readers used the same sequence for each case for pre- and post-ablation measurements.

In conclusion, our study suggests that MW ablation produces more contraction of the ablation zone and tumor compared to RF ablation on immediate post-ablation MRI. The degree of tissue contraction by MW should therefore be taken into account during pre-procedural planning and assessment of treatment response by comparing pre- and post-ablation images.

Compliance with ethical standards

Conflict of interest   None.

References

1. Qian GJ, Wang N, Shen Q, et al. (2012) Efficacy of microwave versus radiofrequency ablation for treatment of small hepatocellular carcinoma: experimental and clinical studies. Eur Radiol . doi: 10.1007/s00330-012-2442-1
2. Fan W, Li X, Zhang L, Jiang H, Zhang J (2012) Comparison of microwave ablation and multipolar radiofrequency ablation in vivo using two internally cooled probes. AJR Am J Roentgenol 198(1):W46–W50. doi:10.2214/AJR.11.6707
3. Lubner MG, Hinshaw JL, Andreano A, et al. (2012) High-powered microwave ablation with a small-gauge, gas-cooled antenna: initial ex vivo and in vivo results. J Vasc Interv Radiol 23(3):405–411. doi: 10.1016/j.jvir.2011.11.003
4. Yu NC, Lu DS, Raman SS, et al. (2006) Hepatocellular carcinoma: microwave ablation with multiple straight and loop antenna clusters–pilot comparison with pathologic findings. Radiology 239(1):269–275. doi:10.1148/radiol.2383041592
5. Ganguli S, Brennan DD, Faintuch S, Rayan ME, Goldberg SN (2008) Immediate renal tumor involution after radiofrequency thermal ablation. J Vasc Interv Radiol 19(3):412–418. doi: 10.1016/j.jvir.2007.10.024
6. Wall MS, Deng XH, Torzilli PA, et al. (1999) Thermal modification of collagen. J Shoulder Elbow Surg 8(4):339–344
7. Yang D, Converse MC, Mahvi DM, Webster JG (2007) Measurement and analysis of tissue temperature during microwave liver ablation. IEEE Trans Biomed Eng 54(1):150–155. doi: 10.1109/TBME.2006.884647
8. Brace CL, Diaz TA, Hinshaw JL, Lee FT (2010) Tissue contraction caused by radiofrequency and microwave ablation: a laboratory study in liver and lung. J Vasc Interv Radiol 21(8):1280–1286. doi: 10.1016/j.jvir.2010.02.038
9. Lubner MG, Brace CL, Hinshaw JL, Lee FT Jr (2010) Microwave tumor ablation: mechanism of action, clinical results, and devices. J Vasc Interv Radiol 21(8 Suppl):S192–S203. doi: 10.1016/j.jvir.2010.04.007
10. Ahmed M, Brace CL, Lee FT Jr, Goldberg SN (2011) Principles of and advances in percutaneous ablation. Radiology 258(2):351–369. doi:10.1148/radiol.10081634
11. Simon CJ, Dupuy DE, Mayo-Smith WW (2005) Microwave ablation: principles and applications. Radiographics 25(Suppl 1):S69–S83. doi:10.1148/rg.25si055501
12. Brace CL, Laeseke PF, Sampson LA, et al. (2007) Microwave ablation with multiple simultaneously powered small-gauge triaxial antennas: results from an in vivo swine liver model. Radiology 244(1):151–156. doi:10.1148/radiol.2441052054
13. Wright AS, Lee FT Jr, Mahvi DM (2003) Hepatic microwave ablation with multiple antennae results in synergistically larger zones of coagulation necrosis. Ann Surg Oncol 10(3):275–283
14. Wolf FJ, Grand DJ, Machan JT, et al. (2008) Microwave ablation of lung malignancies: effectiveness, CT findings, and safety in 50 patients. Radiology 247(3):871–879. doi:10.1148/radiol.2473070996
15. Liang P, Wang Y, Yu X, Dong B (2009) Malignant liver tumors: treatment with percutaneous microwave ablation–complications among cohort of 1136 patients. Radiology 251(3):933–940. doi: 10.1148/radiol.2513081740
16. Orsi MD, Dodd GD 3rd, Cardan RA, et al. (2011) In vitro blood-perfused bovine liver model: a physiologic model for evaluation of the performance of radiofrequency ablation devices. J Vasc Interv Radiol 22(10):1478–1483. doi:10.1016/j.jvir.2011.06.013
17. Merkle EM, Nour SG, Lewin JS (2005) MR imaging follow-up after percutaneous radiofrequency ablation of renal cell carcinoma: findings in 18 patients during first 6 months. Radiology 235(3):1065–1071. doi:10.1148/radiol.2353040871
18. Raman SS, Lu DS, Vodopich DJ, Sayre J, Lassman C (2000) Creation of radiofrequency lesions in a porcine model: correlation with sonography, CT, and histopathology. AJR Am J Roentgenol 175(5):1253–1258
19. Steinke K, King J, Glenn D, Morris DL (2003) Radiologic appearance and complications of percutaneous computed tomography-guided radiofrequency-ablated pulmonary metastases from colorectal carcinoma. J Comput Assist Tomogr 27(5):750–757